Unmanned Helicopter Flight Controller Design by Use of Model Predictive Control

JIANFU DU, YAOU ZHANG, TIANSHENG LÜ
School of Mechanical Engineering
Shanghai Jiao Tong University
800 Dongchuan Rd, Shanghai
CHINA
djf2717@163.com

Abstract: - Helicopters are strongly coupled, multivariate, time-delay nonlinear plants. The design of a stable control system for autonomous flight is a challenging task. But because of wide applications, the research on helicopters is booming. In this paper, we will research on a small scale unmanned helicopter. Firstly, kinematical model and dynamical model are presented. Then we design a flight controller which includes an attitude controller and a position controller. As for attitude control, a novel control method, model predictive control (MPC), is applied. The advantages of MPC are that it can deal with the limits of the actuators and the existing time-delay of the plant. Its performance was verified in real flight experiments. The results show that the controller performs well in position control mode.

Key-Words: - MPC, unmanned helicopter, flight control, helicopter modeling

1 Introduction

Small scale unmanned helicopters offer many advantages, such as low weight and the ability to fly within a narrow space. They can be used in search and rescue after big natural disasters, patrol and surveillance, filming movies, suppression of smuggling, inspection of power lines, large bridges, dams and so on [1].

Many universities, such as Technische Universität Berlin, Georgia Institute of Technology, Stanford, UC Berkley, University of Waterloo etc. are conducting research on autonomous control for small scale unmanned helicopters [2]. There are many control algorithms, such as PID, adaptive nonlinear control, neural networks control, fuzzy control, which can be used in helicopter controller design. But all these methods have one common drawback: They have first to measure the plant output and compare it with the desired output, and then generate the control signal, so the controller output depends on the actual error and short part of the past state trajectory. Compared with these methods, model predictive control generates the control signal based not only on actual error and past state trajectory but also on the future behavior of the system. Even more, the control rules (gains) are changing in every control cycle in order to minimize the control error and satisfy the defined constraints (e.g. limits for controller outputs). For these reasons, a higher computational effort is required, but also superior performance is expected from a model predictive controller even if the model is rough [3].

MPC has widely used not only in process industry, but also in the control of diversity of processes ranging from robot manipulators to clinical anaesthesia. Applications on drying towers, distillation columns, PVC plants, steam generators, motor, etc. have shown MPC can achieve very good performance [4-6]. In [7], R.K. Mehra presented a fuzzy-supervised model predictive controller for tiltrotor aircraft. Simulation results verified its performance. In this paper, the model predictive controller which controls the attitude of the helicopter was applied to a 6 DOFs helicopter. The real flight experiment was carried out to verify the control performance.

This paper is organized as follows. Section 2 reviews multivariate state space model predictive control with constraints and section 3 gives the kinematical and dynamical model of the helicopter. Section 4 presents the proposed control algorithms. The real flight experiments are shown in section 5. Finally, conclusions and future work are outlined in section 6.

2 MPC Algorithm

Model based predictive control makes an explicit use of a model of the plant to obtain the control signal by minimizing an objective function. MPC consists of tree steps: predicting the plant output at a future time moment by use of the plant model, calculating a control sequence by minimizing an objective function, receding, which means that at each moment the horizon is shifted forward, and apply the first control signal of the sequence calculated at each step [4].

MPC can use any kind of model description, e.g. impulse response, step response, transfer function, state space, to predict the plant output. In this paper we use a state space model:

$$\begin{aligned} x(k+1) &= Ax(k) + B\,u(k) \\ y(k) &= C\,x(k) \end{aligned} \quad (1)$$

where, *x(k)* is the n-dimension state vector of the plant, *u(k)* is the m-dimension vector of manipulated variables, *y(k)* is the p-dimension vector of the plant output.

The MPC algorithm minimizes an objective function (2) for obtaining the control law [3]:

$$\min J(k) = \left\| w(k) - y_{PM}(k) \right\|_Q^2 + \left\| \triangle u_M(k) \right\|_R^2 \quad (2)$$

where, *w(k)* is the reference signal,

$$w(k) = \begin{bmatrix} w_1(k) \\ \vdots \\ w_p(k) \end{bmatrix}, \quad w_i(k) = \begin{bmatrix} w_i(k+1) \\ \vdots \\ w_i(k+P) \end{bmatrix}, \quad i = 1, \cdots p$$

$y_{PM}(k)$ is the predictive output,

$$y_{PM}(k) = \begin{bmatrix} y_{1,PM}(k) \\ \vdots \\ y_{p,PM}(k) \end{bmatrix}, \; y_{i,PM}(k) = \begin{bmatrix} y_{i,M}(k+1|k) \\ \vdots \\ y_{i,M}(k+P|k) \end{bmatrix}$$

$$i = 1, \cdots p$$

$$y_{i,M}(k+j|k) = CA^j x(k) + \sum_{g=0}^{j-1} CA^{j-g-1} B \left[u(k-1) + \sum_{h=0}^{g} \triangle u(k+h) \right]$$

$\triangle u_M(k)$ is the differenced input,

$$\triangle u_M(k) = \begin{bmatrix} \triangle u_{1,M}(k) \\ \vdots \\ \triangle u_{m,M}(k) \end{bmatrix}, \; \triangle u_{j,M}(k) = \begin{bmatrix} \triangle u_j(k) \\ \vdots \\ \triangle u_j(k+M-1) \end{bmatrix}$$

$$j = 1, \cdots m$$

$$Q = block - diag(Q_1, \cdots Q_p),$$

$$Q_i = diag\left[q_i(1), \cdots q_i(P) \right], \; i = 1, \cdots, p$$

$$R = block - diag(R_1, \cdots R_m),$$

$$R_j = diag\left[r_j(1), \cdots r_j(M) \right], \; j = 1, \cdots, m$$

P is the cost horizon, and *M* is the control horizon. q_i and r_i are weights that penalize the changes of the error and manipulated variable.

For flight control it is important to limit the absolute and incremental values of plant inputs (actuators) generated by the controller:

$$\begin{aligned} &u_{i,\min} \le u_i(k+j-1|k) \le u_{i,\max} \quad i = 1, \cdots, m; \; j = 1, \cdots M \\ &\triangle u_{i,\min} \le \triangle u_i(k+j-1|k) \le \triangle u_{i,\max} \; i = 1, \cdots, m; \; j = 1, \cdots M \end{aligned} \quad (3)$$

Most controller design methods can not deal explicitly with constraints for plant inputs. Usually, the inputs are simply saturated according to the constraints. In the case of MPC, the input and output constraints can be considered explicitly: The control signal is generated in an optimization procedure considering all defined constraints.

In order to get the optimal control variable $\triangle u_M(k)$, we must solve the equations (1-3). This is a standard quadratic programming (QP) problem of the form:

$$\min \; f(x) = \frac{1}{2} x^T H x + c^T x$$

$$s.t \quad Ax \le b$$

which can be solved e.g. by Lemke algorithms or active set method.[8]

3 Helicopter Modeling

In [9] the main differences between small scale helicopters and full size helicopters are pointed out. These differences are: a much higher ratio of the main rotor mass to fuselage mass in case of the small scale helicopter, the rotation speed of the main rotor of small scale helicopters is higher than of most full size helicopters, and small scale helicopters have very stiff main rotors without flapping hinges. The conclusion was that the inertial effects of the main rotor become the main component influencing the rotational dynamics of the whole mechanical system and the main rotor should be considered as a rigid body not a mass point.

The model of the small scale helicopter is shown in Fig.1. Three PWM servo inputs, s_1, s_2, s_3, control the cyclic pitches of the Bell-Hiller bar (BHB), and the collective pitch of the main rotor P_{col}^{MR} through the lever system L^{MR}. The block A^{MR} describes the aerodynamics of the main rotor. The main rotor generates pitch and roll torques $T_{1,2}^{MR}$, drag torque T_3^{MR} and lifting force F_3^{MR}. The servo input s_5 controls the pitch on the tail rotor through block L^{TR} describing tail rotor servos and lever system. Block A^{TR} describes the aerodynamics of the tail rotor. F_2^{TR} and T_2^{TR} are the force and torque of the tail rotor respectively, generated in A^{TR}. The rotation speed of the engine is controlled by s_4. The outputs of the

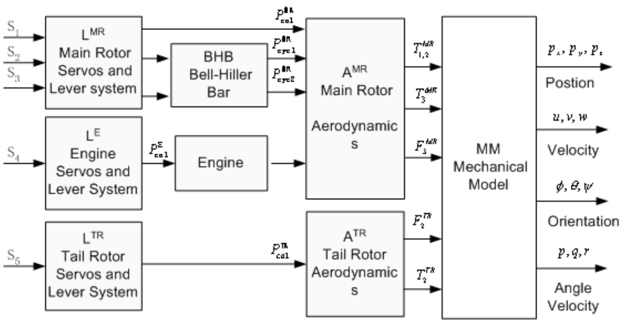

Fig.1. Model of the small scale helicopter

model are: p_x, p_y, p_z ,the position of the helicopter reference point with respect to the inertial system, ϕ, θ, ψ , the yaw-pitch-roll angles describing the orientation of the fuselage relative to the inertial frame, u, v, w , the translational velocity in the inertial frame, and p, q, r , the rotation speeds of the fuselage in the body frame.

In this paper, we use yaw-pitch-roll angles describing the orientation of the fuselage relative to the inertial frame which is different from [9, 10]. The main advantages are the three angles can be controlled separately. If we correct small errors in yaw, roll and pitch individually, then we have achieved the nominal attitude of the aircraft [11].

The blocks A^{MR}, A^{TR} contain models for aerodynamic effects, but they can be approximated with linear functions in the area of operation (this was concluded from experimental results). F_3^{MR} ,$T_{1,2}^{MR}$, F_2^{TR} are linear functions of $P_{\text{col}}^{\text{MR}}$, $P_{\text{cyc1, 2}}^{\text{MR}}$, $P_{\text{col}}^{\text{TR}}$ respectively. The blocks L^{MR}, L^{TR} can be derived using geometrical relationships.

The experiments show that also the effects of the BHB can be approximated with a linear function.
After those significant simplifications, the relationship between servo inputs s_1, s_2, s_3, s_5 and abstract inputs F_3^{MR}, T_1^{MR}, T_2^{MR}, F_2^{TR} can be approximated with linear function, and the coefficients can be identified by experiments.

The kinematical equations and dynamcal equations can be deduced by physical principles.

The kinematical equations for translation are:

$$\begin{aligned} \dot{p}_x &= u \\ \dot{p}_y &= v \\ \dot{p}_z &= w \end{aligned} \tag{4}$$

and for rotation:

$$\dot{\phi} = p + \tan(\theta)(\sin(\phi)q + \cos(\phi)r) \tag{5.a}$$

$$\dot{\theta} = \cos(\phi)q - \sin(\phi)r \tag{5.b}$$

$$\dot{\psi} = (\sin(\phi)q + \cos(\phi)r)/\cos(\theta) \tag{5.c}$$

The translation dynamical equations are derived and have the following form:

$$\begin{aligned} M\dot{u} &= F_3^{MR}(\sin(\phi)\sin(\psi) + \sin(\theta)\cos(\phi)\cos(\psi)) \\ &\quad - F_2^{TR}(\sin(\psi)\cos(\phi) - \sin(\phi)\sin(\theta)\cos(\psi)) \\ M\dot{v} &= F_2^{TR}(\cos(\phi)\cos(\psi) + \sin(\phi)\sin(\theta)\sin(\psi)) \\ &\quad - F_3^{MR}(\sin(\phi)\cos(q6) - \sin(\theta)\sin(\psi)\cos(\phi)) \\ M\dot{w} &= F_2^{TR}\sin(\phi)\cos(\theta) \ + \ F_3^{MR}\cos(\phi)\cos(\theta) \\ &\quad - Mg \end{aligned} \tag{6}$$

The rotation dynamical equations are:

$$\dot{p} = a_{12}q + b_{11}^u T_1^{MR} + b_{11}^v F_2^{TR} + b_{qr}qr \tag{7.a}$$

$$\dot{q} = a_{21}p + b_{22}^u T_2^{MR} + b_{22}^v T_2^{TR} + b_{pr}pr \tag{7.b}$$

$$\dot{r} = \mathrm{b}_{31}^v F_2^{TR} + b_{33}^v T_3^{MR} + b_{pq}pq \tag{7.c}$$

where,

$$a_{12} = -\frac{2M\, I_{11}^{MR}\omega_{MR}}{M(I_{11}^F + I_{11}^{MR}) + (L_F - L_{MR})^2 m_F m_{MR}}$$

$$b_{11}^u = \frac{(L_F m_F + L_{MR}m_{MR})M}{M(I_{11}^F + I_{11}^{MR}) + (L_F - L_{MR})^2 m_F m_{MR}}$$

$$b_{11}^v = \frac{L_{MR}m_{MR}}{M(I_{11}^F + I_{11}^{MR}) + (L_F - L_{MR})^2 m_F m_{MR}}$$

$$b_{qr} = -\frac{M(I_{11}^{MR} - I_{22}^F + I_{33}^F) - (L_F - L_{MR})^2 m_F m_{MR}}{M(I_{11}^F + I_{11}^{MR}) + (L_F - L_{MR})^2 m_F m_{MR}}$$

$$a_{21} = -\frac{2M\, I_{11}^{MR}\omega_{MR}}{M(I_{22}^F + I_{11}^{MR}) + (L_F - L_{MR})^2 m_F m_{MR}},$$

$$b_{22}^u = -\frac{M}{M(I_{22}^F + I_{11}^{MR}) + (L_F - L_{MR})^2 m_F m_{MR}},$$

$$b_{22}^v = -\frac{M}{M(I_{22}^F + I_{11}^{MR}) + (L_F - L_{MR})^2 m_F m_{MR}},$$

$$b_{pr} = -\frac{M(I_{33}^F + I_{11}^{MR} - I_{11}^F) - (L_F - L_{MR})^2 m_F m_{MR}}{M(I_{22}^F + I_{11}^{MR}) + (L_F - L_{MR})^2 m_F m_{MR}}$$

$$b_{33}^v = \frac{1}{I_{33}^F + 2I_{11}^{MR}}$$

$$b_{31}^v = -\frac{L_T}{I_{33}^{FF} + 2I_{11}^{MR}}$$

$$b_{pq} = \frac{I_{11}^F - I_{22}^F}{I_{33}^F + 2I_{11}^{MR}}$$

I_{11}^F, I_{22}^F, I_{33}^F and I_{11}^{MR} are moments of inertial of the fuselage and main rotor in body frame. ω_{MR} is the rotation speed of the main rotor. m_F, m_{MR} are the mass of fuselage and main rotor respectively. L_F is the distance from the mass center of the fuselage to x axis in body frame. L_{MR} is the distance from the center of the main rotor to the origin of the body frame. L_T is the distance from the center of the tail rotor to the origin of the body frame.

4 Controller Design

Similar to other controllers the presented helicopter controller is composed of two nested loops: The inner loop to control the attitude and the outer loop to control the position of the helicopter.

Attitude control

The scheme controlling the attitude angles ϕ,θ is shown in Fig.2. In this scheme, the block Q is composed of the kinematic equations (5), and W is composed of the dynamical equations for rotation (7.a) and (7.b). The block MPC denotes the proposed model predictive controller. In [9], a decoupling block based on inversion of dynamical equations was used, so the accurate knowledge of the model parameters was required. Also the time delay between the controller outputs $T_{1,2}^{MR}$ and corresponding generated torques on the main rotor was not explicitly considered in the controller design. The presented MPC can deal with the coupling and time delay and is robust against parameter variations of the system. In the presented control scheme, the MPC is used for the attitude control, which increases the performance of this important part of the whole controller and makes the position controller more robust.

In order to design the model predictive controller, a model presented in section 3 will be used. Here we consider r equals to 0, F_2^{TR} and T_2^{TR} as disturbances. The equations (7.a)-(7.b) can then be rewritten in the following form:

$$\begin{bmatrix}\dot p\\ \dot q\end{bmatrix}=\begin{bmatrix}0 & a_{12}\\ a_{21} & 0\end{bmatrix}\begin{bmatrix}p\\ q\end{bmatrix}+\begin{bmatrix}b_{11}^u & 0\\ 0 & b_{22}^u\end{bmatrix}\begin{bmatrix}T_1^{MR}\\ T_2^{MR}\end{bmatrix}$$
$$y=\begin{bmatrix}1 & 0\\ 0 & 1\end{bmatrix}\begin{bmatrix}p\\ q\end{bmatrix} \quad (8)$$

The equations above show a strong coupling between two corresponding axes of the helicopter frame. The assumption r=0 is reasonable because there is a separate control loop for r.

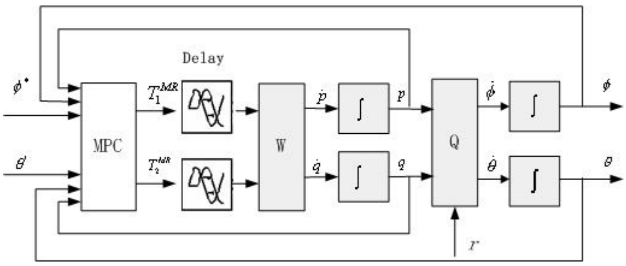

Fig.2. Attitude control

The equation (5.a)-(5.b) can be simplified as follow, if ϕ and θ are very small.

$$\dot\phi = p$$
$$\dot\theta = q \quad (9)$$

Described in state space form:

$$\begin{bmatrix}\dot\phi\\ \dot\theta\end{bmatrix}=\begin{bmatrix}0 & 0\\ 0 & 0\end{bmatrix}\begin{bmatrix}\phi\\ \theta\end{bmatrix}+\begin{bmatrix}1 & 0\\ 0 & 1\end{bmatrix}\begin{bmatrix}p\\ q\end{bmatrix}$$
$$y=\begin{bmatrix}1 & 0\\ 0 & 1\end{bmatrix}\begin{bmatrix}\phi\\ \theta\end{bmatrix} \quad (10)$$

Combining the eqs. (8) and (10), we get the final state space equation:

$$\begin{bmatrix}\dot\phi\\ \dot\theta\\ \dot p\\ \dot q\end{bmatrix}=\begin{bmatrix}0 & 0 & 1 & 0\\ 0 & 0 & 0 & 1\\ 0 & 0 & 0 & a_{12}\\ 0 & 0 & a_{21} & 0\end{bmatrix}\begin{bmatrix}\phi\\ \theta\\ p\\ q\end{bmatrix}+\begin{bmatrix}0 & 0\\ 0 & 0\\ b_{11}^u & 0\\ 0 & b_{22}^u\end{bmatrix}\begin{bmatrix}T_1^{MR}\\ T_2^{MR}\end{bmatrix}$$
$$y=\begin{bmatrix}1 & 0 & 0 & 0\\ 0 & 1 & 0 & 0\\ 0 & 0 & 1 & 0\\ 0 & 0 & 0 & 1\end{bmatrix}\begin{bmatrix}\phi\\ \theta\\ p\\ q\end{bmatrix} \quad (11)$$

The time delay of the plant is 0.12s (found in flight experiments), and both the sampling time and control time are 0.01s. The parameters for the presented controller were chosen as follows: predictive horizon P=40, control horizon M=3. The actuators constraints are defined using the following inequalities:

$$\text{-6 } N.m \le T_1^{MR} \le 6\ N.m$$
$$\text{-6 } N.m \le T_2^{MR} \le 6\ N.m$$

The error weight matrix Q and control weight matrix R were chosen as:

$$Q = block - diag(Q_1, \cdots Q_4),$$

$$Q_1 = Q_2 = diag\left[\underbrace{0,\cdots 0}_{12},\underbrace{10\cdots,10}_{28}\right],$$

$$Q_3 = Q_4 = diag\left[\underbrace{0,\cdots 0}_{40}\right],$$

$$R = block - diag(R_1, R_2),$$

$$R_1 = R_2 = diag\left[0.1, 0.1, 0.1\right]$$

Then we can use QP algorithm to solve the problem.

For the heading angle control a simple P-controller was used. This simple controller works well because the helicopter is equipped with a commercial gyroscope based controller GY401 which can be operated in AVCS mode to keep the helicopter in a fixed heading.

Position control

The position controller is shown in Fig. 3 which consists of a PID block and a F_{123}^{-1} block. The PID block generates the desired acceleration according to the position error. F_{123}^{-1} is the inversion of eq.(6). The *Inner Loop Controlle*r block is an attitude controller which takes desired attitude angle ϕ^*, θ^* as input, and generates the output torques T_1^{MR}, T_2^{MR}. The *Rotation* block converts $T_1^{MR}, T_2^{MR}, T_3^{MR}, F_2^{TR}, T_2^{TR}$ into orientation angles ϕ, θ, ψ . The block F_{123} is translational dynamics which converts orientation angles ϕ, θ, ψ and lifting force F_3^{MR} into acceleration of the translational movement $\dot u, \dot v, \dot w$. Through two integrators the accelerations are integrated to position. Actually the latter grey blocks denote the plant.

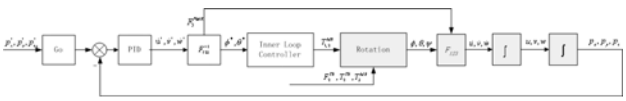

Fig.3. Position Controller

In order to solve the block F_{123}^{-1} , some simplifications are needed to be done. Otherwise, the equation (6) is too complicated to be solved. Here we consider ϕ and θ are very small, then $\cos(\phi) \approx 1, \cos(\theta) \approx 1, \sin(\phi) \approx \theta, \sin(\phi) \approx \theta$. The translational dynamical equation (6) can be rewrite in the following:

$$\begin{aligned} M\dot u &= F_3^{MR}(\phi \sin(\psi) + \theta \cos(\psi)) - F_2^{TR} \sin(\psi) \\ M\dot v &= F_2^{TR} \cos(\psi) - F_3^{MR}(\phi \cos(\psi) - \theta \sin(\psi)) \qquad (12) \\ M\dot w &= F_2^{TR}\phi + F_3^{MR} - Mg \end{aligned}$$

So,

$$\phi = \frac{M(\dot w + g) - F_3^{MR}}{F_2^{TR}}$$

$$\theta = \frac{M(\dot u \cos(\psi) + \dot v \sin(\psi))}{F_3^{MR}}$$

where,

$$F_3^{MR} = \frac{1}{2}M(g + \dot w) + \frac{1}{2}\sqrt{M^2(g+\dot w)^2 + 4F_2^{TR}M(\dot v \cos(\psi) - \dot u \sin(\psi)) - 4F_2^{TR2})}$$

5 Experiments

Hardware of the control system

The control algorithm runs on a small control computer with one 800MHz CPU, one 128M RAM, 2 CAN-bus interfaces, 3 RS-232 interfaces, 1 RS-485 interface, and 1 Ethernet interface. This computer is powerful enough to handle the required complicated mathematical computation of the control algorithms.

The onboard micro controller based on a Siemens SAB80C167 microcontroller deals with the angle velocity signals measured by gyroscopes ADXRS 300 and transferred to the control computer over the CAN-bus interface. The tree-cameras vision system (the three cameras are placed on the ceiling of the lab) measures the position and orientation of the helicopter which is sent to the ground computer through Ethernet. The translation velocities of the helicopter are determined by first order differentiation of the position coordinates

Real flight experiments

The experiments were performed in the laboratory for autonomously flying robot at Technische Universität Berlin. Fig.4 shows the fight scene. The helicopter is fixed in a safecage which is made of carbon tubes and has the mass of 1.2 kg. The four high brightness lamps are used to measure the actual position and orientation of the helicopter by the vision system.

In the flight experiment, the helicopter started at position (0, -1.5, 0.4), then hovered in the position (0, -1.5, 0.9), then moved to the position (0, 0, 0.9), then to (0, -2.5, 0.9), then to (1, -1.5, 0.9). Fig. 5 shows the controller performance. From the figure, we can see that the position precision is about 0.15m which is accurate enough for most practical applications. There is no overshoot and oscillation in the flight also. This is very important in real flight without colliding.

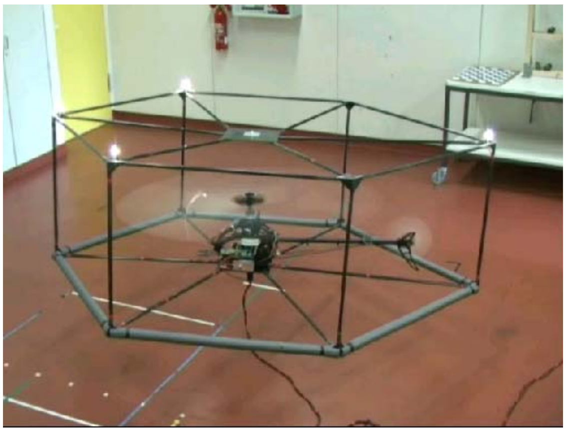

Fig.4. Real flight scene

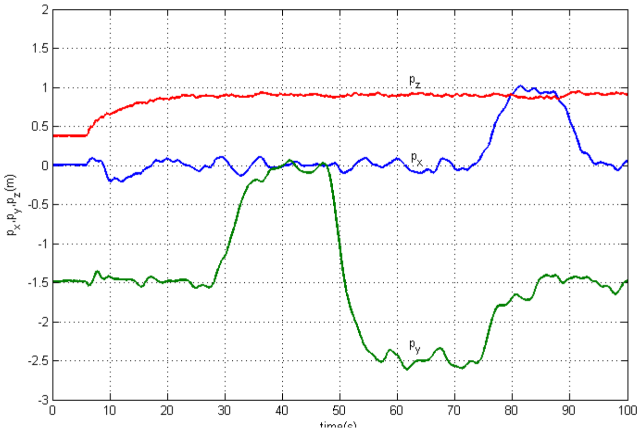

Fig.5. the position of the helicopter using MPC

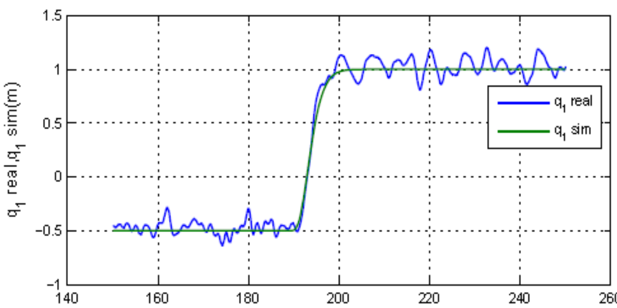

Fig.6. the step response of the helicopter presented in paper [9]

The flight experiment results presented in [9] are also exhibited here for compare. Fig.6 describes the step response of the helicopter. At time t=190s, it changes the position of x axis from -0.5m to 1m. The position precision is about 0.2m. So, comparing with the controller presented in [9], the MPC controller provided better performance.

6 Conclusion

The controller achieves very good performance by using the simplified linear rotational dynamics and the inversion of the dynamical equations for translation. In order to achieve a robust and high performing attitude controller, a model predictive controller was used. The main advantages of the proposed control algorithm are the explicit consideration of time delay and actuator limits in the controller design. In addition, the MPC increases the performance of the closed loop system due to the minimization of the control error using the prediction of the future system behavior.

The real flight experiments verify that the MPC controller used in our control system can work well. The position precision is about 0.15m in position control mode.In the future, we will investigate if the MPC controller for the translational part can increase the performance of the whole closed loop system and do some outdoor experiments to validate the flight controller.

Acknowledgments

This research is a *Project Based Personnel Exchange Programme* (PPP shorted in German) and supported by *German Academic Exchange Service* (DAAD shorted in German) and *China Scholarship Council* (CCS). The authors would like to thank the laboratory for autonomously flying robots at Technische Universität Berlin where the experiments were done. The authors also thank Konstantin Kondak, Markus Bernard, Maximilian Laiacker for the help in real fight experiments and the anonymous reviews for improving the quality of the paper.

References:

[1] D. Fujiawara, K. Nonami, H∞ hovering and guidance control for autonomous small-scale unmanned helicopter, *2004 IEEE/RSJ International conference on intelligent robots and systems*, Sendai, Japan, Vol.3, 2004, pp.2463-2468

[2] IARC, *http://avdil.gtri.gatech.edu/AUVS/IARC LaunchPoint.html*, 2008

[3] Y. Xi, *Model Predictive Control*, National Defence Industry Press, 1993

[4] E. F. Camacho, C. Bordons, *Model Predictive control*, Springer-Verlag, 1999

[5] K. Belda, J. Böhm, Range-Space Modification of Predictive Control for Parallel Robots, *Proceedings of the 3rd WSEAS/IASME International Conference on Dynamical Systems and Control*, Arcachon, France, 2007,

[6] I. I. Siller-Alcalá, et al., Position predictive control for an induction motor, *Proceedings of the 3rd WSEAS/IASME International Conference on Dynamical Systems and Control*, Arcachon, France, 2007, pp.224-228

[7] R. K. Mehra, et al., XV-15 tiltrotor flight control system design using model predictive control, *IEEE Aerospace Conference*, Snowmass at Aspen, CO, USA, Vol.2, 1998, pp.139-148
[8] B. Chen, *The optimization theory and algorithms*, Tsinghua university press, 2004
[9] K. Kondak, et al., Elaborated modeling and control for autonomous small size helicopters, *ISR/ROBOTIK 2006 – Joint conference on robotics*, Munich, 2006,
[10] K. Kondak, et al., Mechanical Model and Control of an Autonomous Small Size Helicopter with a Stiff Main Rotor, *2004 IEEE/RSJ International Conference on Intelligent Robots and Systems*, Vol.3, 2004, pp.2469-2474
[11] Tait-Bryan angles, *http://en.wikipedia.org/wiki/Tait-Bryan_angles*, 2007